

Mover design and characteristics analysis of 2DoF direct drive induction motor

Peixing Wang¹, Jikai Si^{1*}, Haichao Feng¹, Yihua Hu², Wenping Cao³

¹ School of Electrical Engineering and Automation, Henan Polytechnic University, Jiaozuo Henan, China

² Department of Electrical Engineering and Electronics, University of Liverpool, Liverpool, UK

³ University of Aston, Department of Electrical Engineering, Birmingham, UK

* sjjikai527@126.com

Abstract: Two degree-of-freedom direct drive induction motor (2DoFDDIM), capable of rotary, linear and helical motion, has widespread application. A new mover structure is proposed, which is made from a hollow cylinder with copper cast in the axial slots and the circumferential slots on its surface. Then 3D finite element models of 2DoFDDIM are used to determine the performances of rotary, linear and helical motion developed by the motor. The results show that the new mover has a great improvement on the motor performances of all modes of motion compared to the initial mover. The researches on mover structure and characteristics of 2DoFDDIM present a new path of optimization on 2DoF induction motor.

1. Introduction

2DoF induction motor (2DoFIM) is capable of rotary, linear and helical motion without gears. With advantages such as small size, high integrations and efficiency, and so on, it has a widespread application in special industrial fields for drill press, carving machine, boring machines and grinders [1, 2].

Certain types of 2DoFIMs have been developed over the years, and scholars and specialists in various countries have been made important contributions to the structure design, theoretical analysis, coupling magnetic field and control strategies of 2DoFIM [3-8]. The two-armature rotary-linear induction motor with the armatures axially connected in series was analyzed [3-5]. As indicated by the analysis on the motor characteristics through finite element and frequency domain sliding technology, the linear magnetic field and linear motion could weaken the rotary torque and efficiency to some extent. The composite multilayer method, which is simpler and quicker than finite element method [6], was applied to the analysis and performance calculation of the 2DoFDDIM. The computational accuracy of the composite multilayer method is able to fulfill the accuracy requirements compared to finite element method and measured results. A new concept, named static coupling effect [7], focused on the coupling magnetic field in 2DoFDDIM, is put forward. The influence factors and change rule was

analyzed by 3D finite element model.

For most 2DoFIMs, with benefits such as simple, cheapness and strength, a cylinder-shaped solid mover is widely adopted [3-11]. However, similar to the traditional solid rotor induction motors, solid mover causes low power factor, high mover loss and poor efficiency that seriously affects the application of 2DoFIMs.

In the research of traditional solid induction motors, by designing the rotor structure such as slot or slot with copper cast in slots to modify the air-gap magnetic field, the motors' performances are improved [12-17]. In [13], the additional torque caused by slot ripples has been researched. The rotor with the pear-shaped slot is the most inhibition to slot ripples compared to the rotors with the circular slot and trapezoidal slot, which is verified by finite element method. In addition, the number, depth and width of the slots will affect the performances of the motor by the change of the equivalent impedance of the rotor [14, 15]. In [16, 17], the loss of the rotor with axial slot and copper end ring has been studied. Through radial grooving of the rotor surface and thereby cutting the path for high frequency rotor harmonic currents, the eddy current loss and temperature of the rotor can be reduced numerically and experimentally. Numbers of studies had verified that slotting on the solid rotor has great influence on the performances of the motor.

For reducing the mover loss and improving the performances of 2DoFDDIM, a novel mover, which is

slotted along the axial and circumferential direction on a smooth solid mover surface first and copper is cast in the slots (SWCCM), is first proposed in this paper. This mover will change the distribution of air-gap magnetic field and modify the distribution of mover eddy current, which resulting a better performances. And the 3D finite element models of 2DoFDDIM with the initial mover and the novel mover are established. The usability and the feasibility of the SWCCM are first simulated by FEM. Then, the performances such as mover loss, torque (or force), current and so on in rotary, linear and helical motion are all simulated and compared.

2. Structure and principles of operation

The initial 2DoFDDIM consists of a rotary arc-shaped armature in the rotary part, a linear arc-shaped armature in the linear part and a cylinder-shaped solid mover coated with copper layer shared by the two parts. The rotary part stator core is slotted along the axial direction but the linear part stator core is slotted along the circumferential direction. The structure of 2DoFDDIM is shown in Fig. 1. The main structure parameters are summarized in Table 1.

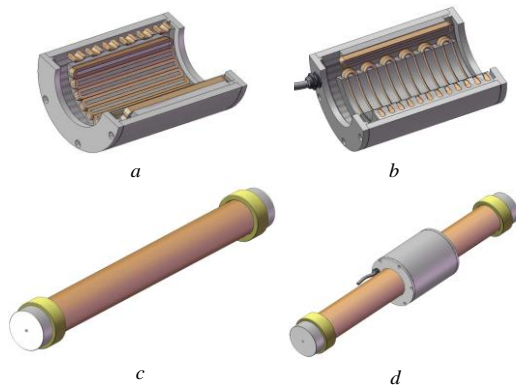


Fig. 1 Structure of 2DoFDDIM

a Rotary arc-shaped armature

b Linear arc-shaped armature

c Solid mover

d Assembly of the 2DoFDDIM

Table 1 Structure parameters of 2DOFDDIM

| Items of interest | Values/dimension | |
|-------------------|------------------|-------------|
| | Rotary part | Linear part |
| Rated voltage | 220 V | 220 V |

| | | |
|------------------------|--------|--------|
| Supply frequency | 50 Hz | 50 Hz |
| Pole pires | 2 | 2 |
| Stator inner diameter | 98 mm | 98 mm |
| Stator outer diameter | 155 mm | 155 mm |
| Stator axial length | 156 mm | 156 mm |
| Air-gap thickness | 2 mm | 2 mm |
| Mover outer diameter | 94 mm | |
| Mover axial length | 600 mm | |
| Copper layer thickness | 1 mm | |

According to the mode of the power supply, 2DoFDDIM can be able to produce different forms of air-gap magnetic fields and generate the corresponding electromagnetic force on the mover surface to directly drive the mover to do rotary, linear, or helical motion^[11].

3. A novel mover structure and principles of operation

In order to reduce the mover loss and improve the motor performances, a novel mover applied to 2DoFDDIM is proposed. Firstly, the axial slots and the circumferential slots are slotted simultaneously on a hollow steel cylinder surface. And then the slot-shaped copper bars are cast and arranged in the slots. The interfaces of axial part and circumferential part are welded by copper to retain low-resistance connections, finally. The structure of the SWCCM is shown in Fig. 2. The shape, width and depth of the axial slots are same as the circumferential slots, whilst the number of axial slots under the rotary arc-shaped armature is equal to that of circumferential slots under the linear arc-shaped armature. The parameters of the SWCCM are listed in Table 2.

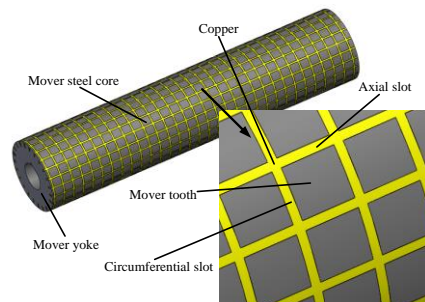


Fig. 2 The ctructure of the SWCCM

Table 2 The parameters of the SWCCM

| Items | Parameters |
|----------------|--|
| Outer diameter | 94 mm |
| Axial length | 600 mm |
| Slot width | 2 mm |
| Slot depth | 7 mm |
| Slot pitch | 10.84 mm(axial) 11.57 mm(circumferential) |

When the rotary part and the linear part of 2DoFDDIM are powered, the air-gap magnetic field consists of a rotary motion magnetic field and a linear motion magnetic field. Due to the difference of permeability and conductivity between the mover steel core and slots, the magnetic field will through the mover teeth and yoke to form a magnetic circuit, and the mover eddy current will almost focus on the slots to form an eddy circuit. The local equivalent model of the SWCCM, which shows the distribution of the magnetic field and the induced current, is shown in Fig. 3.

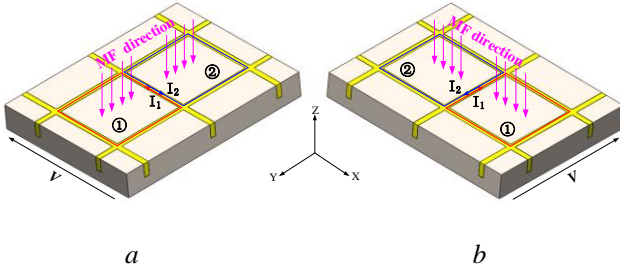


Fig. 3 The local equivalent model of the SWCCM

a Rotary part

b Linear part

For the rotary part of 2DoFDDIM, in the circumferential slot between the two neighboring teeth in the axial direction, the induced current density is expressed by

$$J_c = \frac{1}{A_s R} \int_S \frac{\partial(B_1 - B_2)}{\partial t} \cdot dS \quad (1)$$

Where A_s express the sectional area of the circumferential slot, R is the resistance of the copper around a tooth, S is the superficial area of a tooth, B_1 and B_2 are the magnetic flux density through the two teeth, respectively.

Due to $B_1 = B_2$, $J_c = 0$ can be concluded. In a word, there is no induced current flowing across the

circumferential slot between the two neighboring teeth in axial direction under the range of the rotary motion magnetic field. And the induced current will flow across the axial slots and the circumferential slots on the two sides to form an eddy current circuit. There is no circumferential component of the rotary part eddy current under the rotary motion magnetic field range.

Similar, the linear part eddy current, which flow across the circumferential slots and the axial slots on the two sides of the linear motion magnetic field, is generated. And there is no axial component of the linear part eddy current under the linear motion magnetic field range.

In a word, when the SWCCM is adopted, under the action of the air-gap magnetic field, the corresponding eddy currents were generated. Then, the rotary torque or the linear force or all of them were produced to drive the mover to do rotary, linear or helical motion.

4. 3D finite element analysis

4.1 Magnetic field and eddy current field

According to the structure and parameters of 2DoFDDIM and the SWCCM, the 3D finite element model of 2DoFDDIM with the SWCCM was established in *Magnet*, as shown in Fig. 4. The rotary part and the linear part of 2DoFDDIM are energised by a 220V, 50Hz three-phase AC source, respectively.

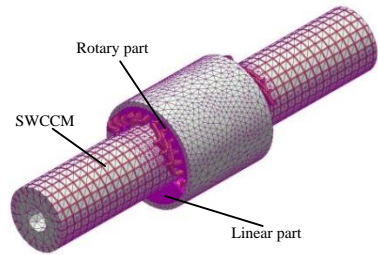


Fig. 4 The 3D finite element model of 2DoFDDIM with the SWCCM

Based on the 3D finite element model, the performances of 2DoFDDIM with the SWCCM can be predicted by finite element method. The distributions of magnetic field and eddy current field of the SWCCM when the mover is locked are shown in Fig. 5.

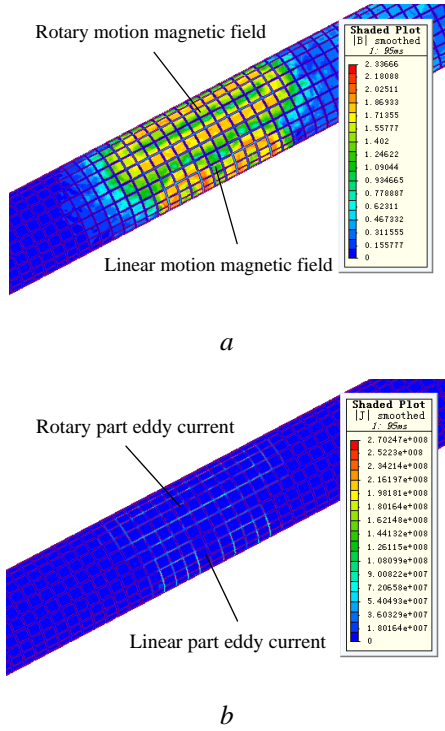


Fig. 5 The distribution of the magnetic field and the eddy current of the SWCCM
a Magnetic field
b Eddy current field

As shown in Fig. 5a, the air-gap magnetic field, no matter the rotary motion magnetic field or the linear motion magnetic field, are all pass through the mover teeth and yoke. And it can be found that there is almost no magnetic field in the slots. As shown in Fig. 5b, the rotary part eddy current field, corresponding to the rotary motion magnetic field, is almost concentrated in the axial slots. And the linear part eddy current field, corresponding to the linear motion magnetic field, is almost concentrated in the circumferential slots. The distributions of the air-gap magnetic field and the eddy current field are in agreement with the analysis in the third part. Hence, by the interaction between the magnetic field and the eddy current field, the rotary torque and the linear force will be produced to drive the mover to do helical motion. On the conditions of the rotary part loads 5Nm and the linear part loads 80N, the waveforms of rotary torque and the linear force are shown in Fig. 6a, and the speed curves are shown in Fig. 6b.

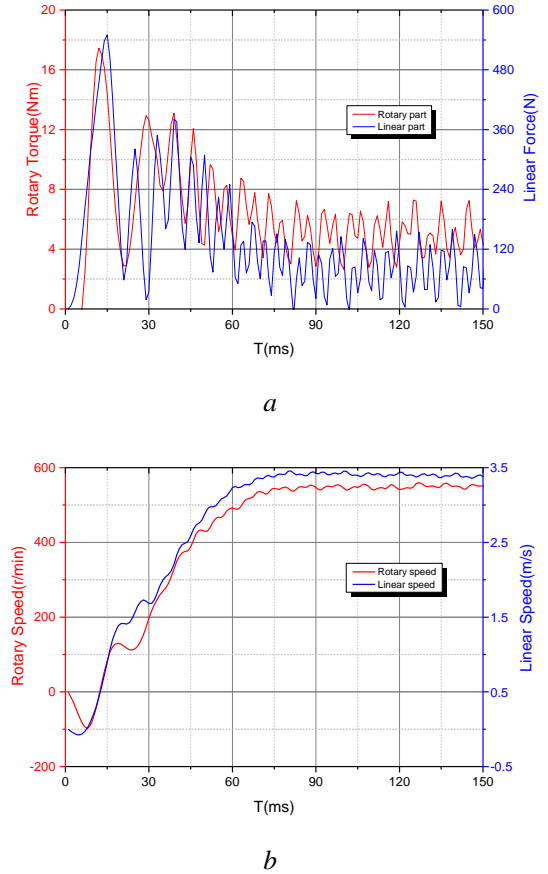


Fig. 6 The characteristics of 2DoFDDIM with the SWCCM
a The curves of electromagnetic force
b The curves of speed

From the Fig. 6, the SWCCM is able to do helical motion, which verifies that the SWCCM satisfies the demand of 2DoF motion and can be applied to 2DoFDDIM.

4.2 Mover loss

For the initial structure of 2DoFDDIM, the mover loss is a major hazard to the safe operation of 2DoFDDIM. When the original mover applies to 2DoFDDIM, two 220V, 50Hz three-phase AC sources are energised for the linear part and the rotary part, respectively. The distributions of magnet field and eddy current field of the SWCLM when the mover is locked are shown in Fig. 7. The value of magnetic field and eddy currents are listed in Table 3.

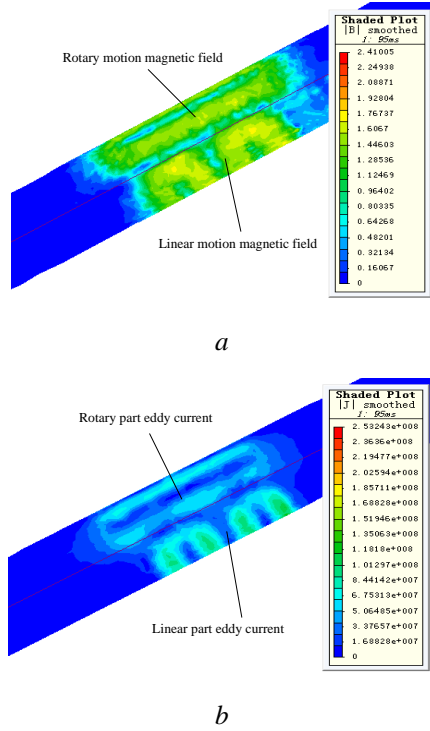


Fig. 7 The distributions of magnetic field and eddy current of 2DoFDDIM with SWCLM
a Magnetic field
b Eddy current

Table 3 The value of magnetic field and eddy currents

| Items | | SWCLM | SWCCM | Variance |
|--------|-------------------------------|-------|-------|----------|
| Rotary | B (T) | 1.104 | 1.362 | +23.26% |
| part | J (10^7 A/m ²) | 5.811 | 1.597 | -72.51% |
| Linear | B (T) | 1.190 | 1.485 | +24.79% |
| part | J (10^7 A/m ²) | 6.818 | 1.916 | -71.90% |

From Fig. 7b and Fig. 5b, it can be concluded that the rotary part eddy current of SWCLM contains more circumferential component and the linear part eddy current contains more axial component compared to SWCCM, which will heighten the fluctuation of the mover. From Table 3, in the conditions of same power source and operating point, it can be concluded that the rotary motion magnetic field of the SWCCM is 23.26% stronger and the linear motion magnetic field of the SWCCM is 23.79% stronger than that of the SWCLM. In addition, the rotary part eddy current of the SWCCM reduces by 72.51% and the linear part eddy current of the SWCCM reduces by 71.90% compared with that of the SWCLM.

The mover loss of 2DoFDDIM, consisting of more than 98% of ohmic loss and a little iron loss, which dissipates in the form of heat to make a high temperature rise, is simulated by 3D finite element method. With the same change of the rotary part slip and linear part slip, the mover losses of the SWCLM and the SWCCM are shown in Fig. 8a and Fig. 8b, respectively. The ratio of them is shown in Fig. 9, which is expressed by

$$K = \frac{P_{swccm}}{P_{swclm}} \quad (3)$$

Where P_{swccm} is the mover loss of the SWCCM and P_{swclm} is the mover loss of the SWCLM.

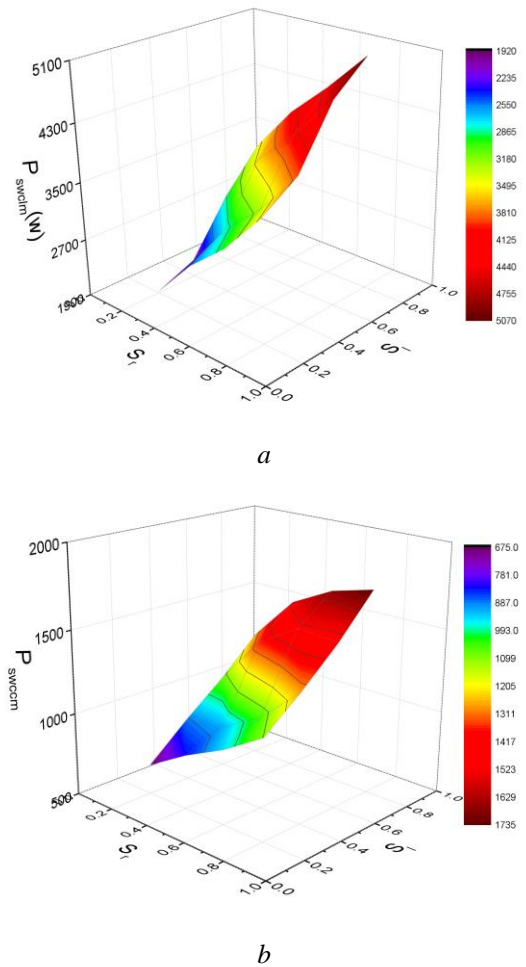


Fig. 8 The mover loss of 2DoFDDIM
a Mover loss of the SWCCM
b Mover loss of the SWCLM

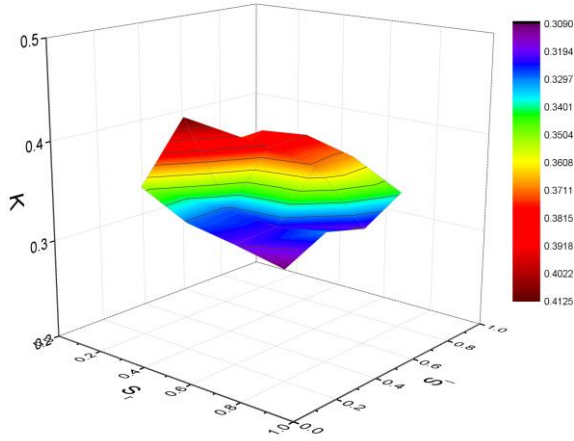


Fig. 9 The ratio of the two mover loss

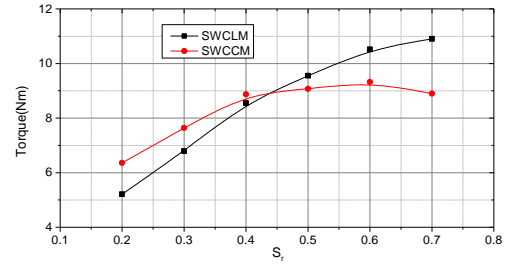
From Fig. 8a and Fig. 8b, no matter what the mover is, the mover loss of 2DoFDDIM gets bigger with the increase of the slips. The high mover loss of the SWCLM results a high temperature rise, which deteriorates the operation of 2DoFDDIM. The mover loss of the SWCCM decreases more than halved (ranging from 58.8% to 69.1%) compared with the SWCLM, which can be concluded from Fig. 9.

In a word, the SWCCM, which has a great effect on reducing the mover loss and thereby reducing the mover temperature, is propitious to the safe operation and the performances of 2DoFDDIM.

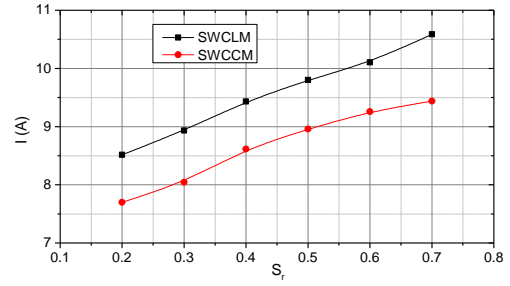
4.3 Characteristic analysis

It has been verified that the SWCCM, which satisfies the demand of 2DoF motion, has a significant effect on reducing the mover loss when applied to 2DoFDDIM. Besides, whether the other performances of 2DoFDDIM are improved or not remains to be researched.

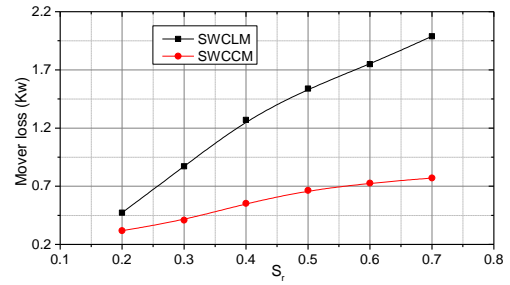
2DoFDDIM has three modes of motion according to the modes of power supply. The performances of 2DoFDDIM under different motions are different. First, the rotary and linear performances of 2DoFDDIM with different movers are simulated. The rotary torque, armature current, mover loss and efficiency of the rotary part when 2DoFDDIM only does rotary motion are shown in Fig. 10. The similar performances of the linear part when there is only linear motion produced are shown in Fig. 11.



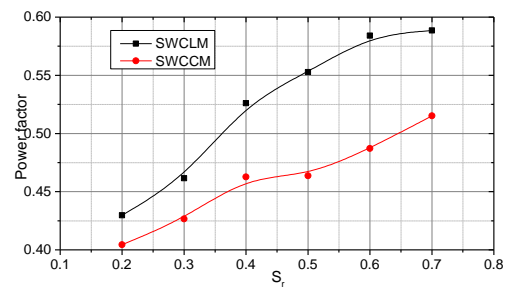
a



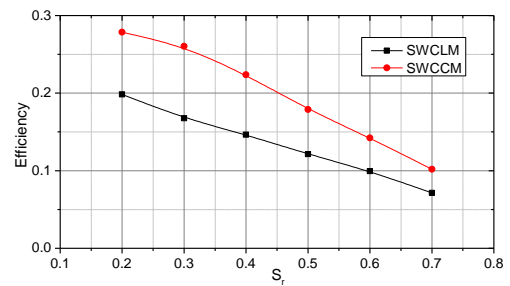
b



c



d



e

Fig. 10 The performances of 2DoFDDIN rotary part

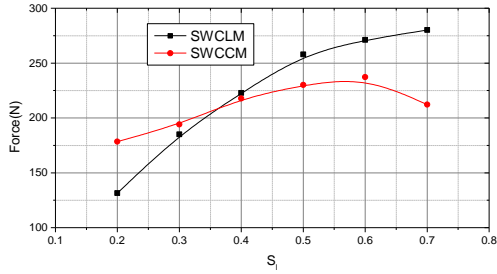
a $T-S_r$

b $I-S_r$

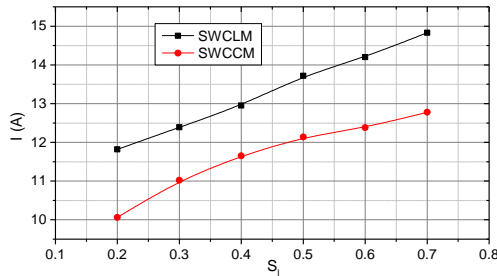
c Mover loss- S_r

d Power factor- S_r

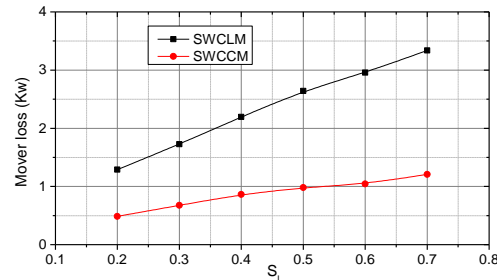
e Efficiency- S_r



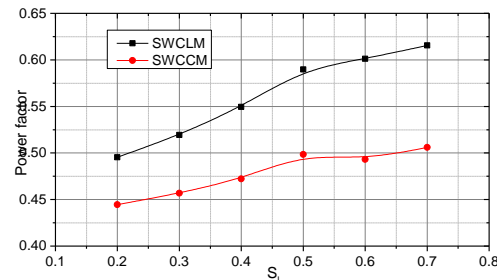
a



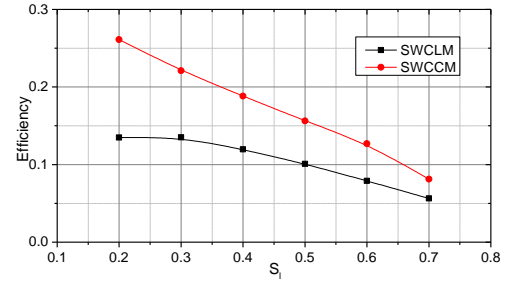
b



c



d



e

Fig. 11 The performances of 2DoFDDIN linear part

a $F-S_l$

b $I-S_l$

c Mover loss- S_l

d Power factor- S_l

e Efficiency- S_l

Where the S_r is the slip of rotary part and the S_l is the slip of linear part.

From Fig. 10a and Fig. 11a, the $T-S_r$ curve of rotary part is similar to the $F-S_l$ curve of linear part no matter what the mover structure is. The torque of rotary part (or the force of linear part) of the 2DoFDDIM with the SWCCM increases first and then decreases, but the torque of rotary part (or the force of linear part) of the 2DoFDDIM with the SWCLM increases as the slip increases. The torque of rotary part of the SWCCM is bigger than that of the SWCLM when rotary part slip $S_r < 0.45$, and smaller when rotary part slip $S_r > 0.45$. The force of linear part of the SWCCM is bigger than that of the SWCLM when linear part slip $S_l < 0.35$, and smaller when linear part slip $S_l > 0.35$. The equivalent impedance of the SWCCM is smaller than that of the SWCLM, which in terms of the change of $T-S_r$ and $F-S_l$ of the two movers, whilst there is a breakdown slip of the curves of the SWCCM.

Comparison of Fig. 10b with Fig. 11b, Fig. 10c with Fig. 11c, Fig. 10d with Fig. 11d, it can be concluded that the armature currents, the mover loss and the power factor of rotary part and linear part increase as the slips increase. The armature currents reduce markedly after applying the SWCCM, where the armature current of rotary part reduces by 9.33% and the linear part reduces by 12.4% in average. It can be concluded that the mover loss reduces by 53.1% when only rotary motion and

reduces by 62.6% when only linear motion after replacing the SWCLM with the SWCCM. However, the power factor with the SWCCM reduces by 11.8% in average of rotary part and 14.6% of linear part compared to the SWCLM.

From Fig. 10e and Fig. 11e, the efficiencies decrease as the slips increase in the simulation range. The efficiency of rotary part with SWCCM is 1.47 times in average of the case with SWCLM. And the number reaches to 1.62 for linear part.

When there is only single-freedom motion produced, the armature currents and the mover loss have a significant reduction while the rotary torque (or linear force) have a considerable increase at smaller slip when the SWCCM is adopted. Although the power factor decreases a little, the efficiency has been enhanced greatly. In a word, in normal operating conditions of single-freedom motion, there is great improvement on the performances of 2DoFDDIM rotary part and linear part after adopting the SWCCM.

When 2DoFDDIM does helical motion, the mover loss greatly reduces after changing the SWCLM to the SWCCM, which has been verified by the comparison of Fig. 8a with Fig. 8b. Due to the intercoupling of the 2DoF magnetic field and motion, there is a compromise between the performances of rotary part and linear part, when 2DoFDDIM does helical motion. The loads that a suitable load 5Nm for rotary part and a light load 80N for linear part, or a light load 3Nm for rotary part and a suitable load 150N for linear part, which making the motor operat at smaller slips, are selected. The performances of 2DoFDDIM with different loads are summarized in Table 4 and Table 5, respectively.

Table 4 The performances of 2DoFDDIM with load 5Nm-80N

| Items of interest | Load 5Nm-80N | | | |
|-------------------|-----------------|-------------|-------------|---------|
| | SWCLM | SWCCM | variance | |
| Rotary part | Average torque | 4.81 Nm | 4.99 Nm | +3.81% |
| | Starting-torque | 15.06 Nm | 17.45 Nm | +15.87% |
| | current | 8.77 A | 8.20 A | -6.50% |
| | Speed | 418.7 r/min | 549.7 r/min | +31.30% |
| | Fluctuation | 10.1 | 7.15 | -29.21% |
| Linear | Average force | 71.35 N | 75.83 N | +6.28% |

| | | | | |
|------|-----------------|----------|----------|---------|
| part | Starting-torque | 371.55 N | 550.08 N | +48.05% |
| | current | 11.58 A | 11.31 A | -2.36% |
| | Speed | 3.12 m/s | 3.39 m/s | +8.82% |
| | Fluctuation | 13.0 | 6.0 | -53.83% |
| | Power loss | 3224 W | 2814 W | -12.7% |

Table 5 The performances of 2DoFDDIM with load 3Nm-150N

| Items of interest | Load 3Nm-150N | | | |
|-------------------|-----------------|-------------|------------|---------|
| | SWCLM | SWCCM | variance | |
| Rotary part | Average torque | 2.66 Nm | 2.73 Nm | +2.63% |
| | Starting-torque | 12.6 Nm | 14.21 Nm | +12.87% |
| | current | 8.66 A | 7.74 A | -10.62% |
| | Speed | 525.4 r/min | 645.1r/min | +22.78% |
| | Fluctuation | 9.235 | 7.754 | -16.03% |
| Linear part | Average force | 143.82 N | 150.23 N | +4.47% |
| | Starting-torque | 444.8 N | 522.5 N | +17.47% |
| | current | 11.85 A | 11.31 A | -4.59% |
| | Speed | 2.44 m/s | 2.64 m/s | +8.24% |
| | Fluctuation | 4.95 | 4.67 | -45.97% |
| Power loss | 3140 W | 2768 W | -11.8% | |

Form the performances data in Table 4 and Table 5, after changing the SWCLM to the SWCCM, the torque (or force), starting-torque(or starting-force) and speed are all enhanced, resulting stronger load-bearing capacity and starting performance of 2DoFDDIM. The speed fluctuations decrease a lot with the two different loads which correspond to the section 4.2. Besides, the power loss with the SWCCM is smaller in excess of 10% compared to the case with the SWCLM. These results verify that the SWCCM can greatly improve the helical motion performances of 2DoFDDIM.

According to the above simulation results and analysis, the SWCCM has greatly improvement on the performances of 2DoFDDIM at all motion states by reducing the mover loss, armature currents and fluctuations, while increasing electromagnetic force. Besides, the load-bearing capacity and starting performance of 2DoFDDIM are improved too. These results confirm that the performances of 2DoFDDIM can be improved by designing the mover structure.

5. Conclusion

2DoFDDIM is one of a solid mover induction motors with two degrees of mechanical freedom. The original mover of 2DoFDDIM has so high mover loss which verified by finite element method.

In this paper, a novel structure mover applying to 2DoFDDIM was proposed. The usability and the feasibility of the SWCCM were analyzed and verified by FEM. The performances of 2DoFDDIM with the SWCCM, such as mover loss, current, torque (or force) and so on, were simulated and compared with that of the SWCLM. The results indicated that the SWCCM satisfies the demand of 2DoF-motion and has a great effect on reducing the mover loss and armature currents.

The research in this study verifies the feasibility of improving the performances of 2DoFDDIM by designing the mover structure and opens a new path for optimization on 2DoFDDIM.

6. Acknowledgments

This work is supported by National Natural Science Foundation of China under grant 51277054, Project of Key Scientific and Technological Research in Henan Province 152102210101, Henan Natural Science Foundation of China under grant 162300410117.

7. References

- [1] Li, S. Y., and Cheng, K. W.: 'A New Two-degree of Freedom Switched Reluctance Motor for Electric Vessel', 6th International Conference on Power Electronics Systems and Applications (PESA), Hong Kong, 2015, pp. 1–6.
- [2] S. Yasukazu.: 'Development of 2-degree-of-freedom rotational/linear switched reluctance motor', IEEE Trans. Magnetics., 2007, 6, (43), pp. 2564-2566.
- [3] Amiri E, Jagiela M, Dobzhanski O, et al.: 'Modeling Dynamic End Effects in Rotary Armature of Rotary-Linear Induction Motor'. In *2013 IEEE International Electric Machines & Drives Conference (IEMDC)*, 2013.
- [4] Amiri, Ebrahim.: 'Circuit Modeling of Double-Armature Rotary-Linear Induction Motor'. In *IECON 2014 - 40th Annual Conference of the IEEE Industrial Electronics Society*, 2014.
- [5] Amiri E, Gottipati P, Mendrela E A.: '3-D Space Modeling of Rotary-Linear Induction Motor with Twin-Armature'. In *2011 1st International Conference on Electrical Energy Systems (ICEES)*, 2011.
- [6] Si J, Xie L, Cao W, et al.: 'Performance analysis of the 2DoF direct drive induction motor applying composite multilayer method'. IET Electric Power Applications, 2017, 11, (4), pp. 524~531.
- [7] Si J, Xie L, Xu X, et al.: 'Static coupling effect of a two-degree-of-freedom direct drive induction motor'. IET Electric Power Applications, 2017, 11, (4), pp. 532~539.
- [8] Si J, Ai L, Xie L, et.: 'Analysis on Electro-magnetic Field and Performance Calculation of 2-DOF Direct Drive Induction Motor'. Transactions of China Electrotechnical Society, 2015, 14, pp. 153-160.
- [9] Alwash J H H, Mohssen A D, Abdi A S.: 'Helical motion tubular induction motor'. IEEE Transactions on Energy Conversion, 2003, 18, (3), pp. 362~369.
- [10] Si J, Si M, Xu X, et.: 'Effects of rotor condition material and air gap length on performance of linear arc-shaped induction motor'. Electric machines and control, 2012, 10, pp. 31-37.
- [11] Si J, Feng H, Ai L, et al.: 'Design and Analysis of a 2-DOF Split-Stator Induction Motor'. IEEE Transactions on Energy Conversion, 2015, 30, (3), pp. 1200~1208.
- [12] Huang Z, Wang S, Sun Y, et.: 'Equivalent-circuit Parameter Calculations and Performance Analysis of Slit Solid Rotor Asynchronous Machines'. Proceedings of the CSEE, 2017, 4, pp. 1208-1215.
- [13] Zhang K, Jiang X, Wu Y.: 'Effect of Slot Shape in Rotor of Electrical Motor with High-Speed Spindle on Slot ripples'. In *Proceedings of the 2010 International Conference on Modelling, Identification and Control*, 2010, pp. 670-675.
- [14] Huang Z, Wang S, Ni S.: '2D Calculation Methods of Equivalent-circuit Parameters in Smooth Solid Rotor Induction Machines'. Proceedings of the CSEE, 2016, 0, pp. 1-8.
- [15] Niazazari M, Mirsalim M, Mohamadi S. Effect of rotor slots parameters on synchronization capability of slotted solid rotor line start permanent magnet motor. 4th Power Electronics, Drive Systems & Technologies Conference (PEDSTC2013), Tehran, Iran, Feb, 2013.
- [16] Gessese Y, Binder A. Axially Slitted, High-Speed Solid-Rotor Induction Motor Technology with Copper End-Rings. In *ICEMS*, 2009.
- [17] Gessese Y, Binder A, Funieru B. Analysis of the effect of radial rotor surface grooves on rotor losses of high speed solid rotor induction motor. IEEE International Symposium on Power Electronics, Electrical Drives, Automation and Motion, 2010, pp. 1762~1767.